Impact of near-surface topography on reflection distortions: From diffractions to speckle noise

Akshika Rohatgi, Andrey Bakulin, Sergey Fomel, Bureau of Economic Geology, University of Texas at Austin, and Jacob Badger, University of Texas at Austin, FrequenSol, LLC*

Summary

Near-surface complexity in land environments creates persistent distortions in seismic wavefields, compromising the fidelity of reflection imaging. Using controlled numerical simulations helps isolate and analyze the propagation-based distortions caused by realistic topographic heterogeneity, specifically rough weathered-bedrock interfaces. By progressively varying the roughness scale in an acoustic finite-element model, we track the emergence of transmission-induced diffraction events that ride along the reflection path. With medium-scale heterogeneity, these distortions appear as diffraction hyperbolas that mimic and obscure primary reflections. As the heterogeneity becomes finer and more densely packed, these diffractions merge into a speckle regime, producing phase randomization that intensifies with frequency. These reflection-coupled distortions affect all subsurface reflectors regardless of depth, offering a plausible mechanism behind observed noise effects in complex near-surface areas.

Introduction

Land seismic data are notoriously complex due to the intricate and heterogeneous nature of the near-surface. The near-surface consists of unconsolidated sediments, weathered layers, topographic variations, and anthropogenic features (Yilmaz, 2001). Despite extensive research, the variety of contributing factors-particularly in elastic or viscoelastic regimes-continues to cloud our understanding of these distortions. Many authors, including Stork (2020, 2024), point to the elastic wavefield as a dominant source of this complexity.

Seismic reflection data processing primarily focuses on extracting primary reflections from deeper subsurface structures. Bakulin et al. (2022a, 2022b) identified a specific distortion mechanism that does not require elastic effects per se: speckle scattering noise. This phenomenon arises from forward ballistic small-scale near-surface scatterers and results in propagation-based distortions that universally affect all reflections-strong or weak, shallow or deep. Though only one of many distortion types, it is uniquely impactful because it imprints every seismic event that traverses the near surface. Prior studies have focused on volumetric small-scale scatterers and their role in generating statistically behaving speckle noise.

In this study, we expand that framework by investigating another class of near-surface heterogeneity: rough geological boundaries, such as the interface between weathered and unweathered rock (Phillips et al., 2019). We systematically explore the impact of the scale of these topographic variations, ranging from large to small relative

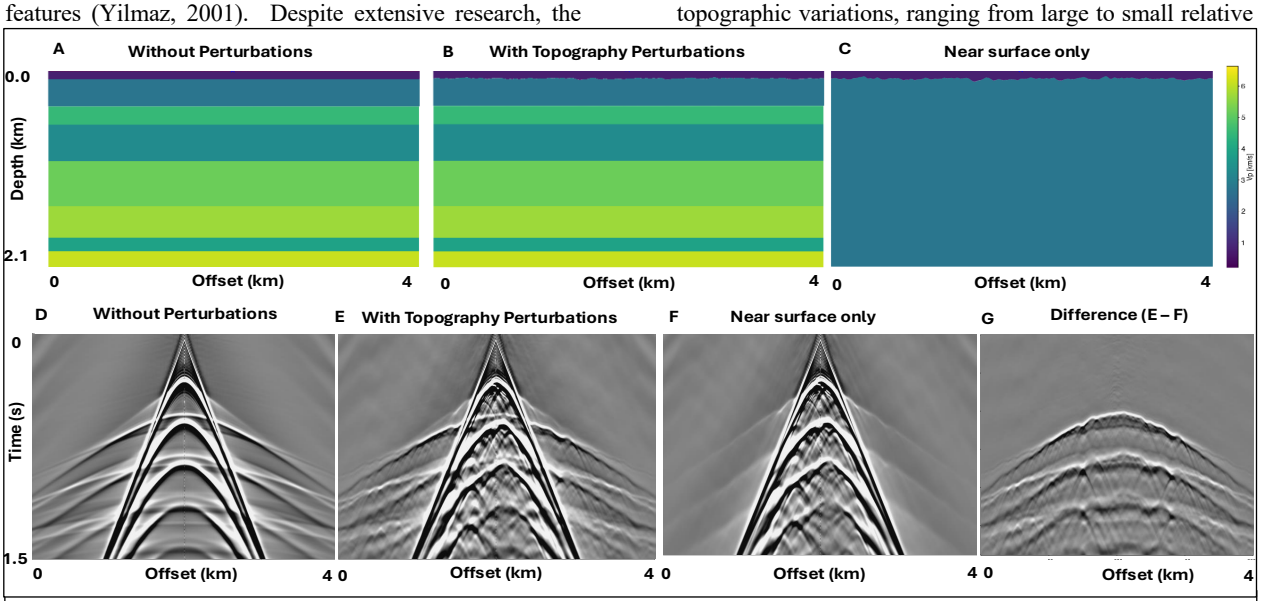

Figure 1: (A-C) Velocity models: (A) Baseline smooth-layered model; (B) Same model with rough topography simulating a weathered-bedrock interface; (C) Rough surface over a homogeneous medium to isolate near-surface contributions. (D-F) Simulated wavefields: (D) Clean reflections from the unperturbed model; (E) Reflections with distortions from surface roughness; (F) Wavefield with near-surface effects alone, without deeper reflections. (G) Residual wavefield from (E - F), isolating propagation-induced distortions on deeper reflections.

10.1190/image2025-4316605.1

to the seismic wavelength, on wavefield distortions. Starting from a simple acoustic layered model, we progressively introduce surface roughness to simulate increasing levels of heterogeneity. We employ FrequenSolve, a novel finite element modeling code featuring a scalable and efficient frequency-domain solver (Badger et al., 2024a,b). This controlled setup allows us to observe a clear transition from isolated diffraction patterns at large scales to overlapping diffractions at intermediate scales and finally to a speckle regime when heterogeneities become densely packed. We analyze the resulting wavefields and seismic phases to quantify the cumulative impact of these topographic features on deeper reflectors.

Effect of near-surface topography on seismic reflections

We designed a controlled modeling experiment to isolate the impact of near-surface topography on seismic reflections. We started with a simple layered acoustic velocity model (Figure 1A) and simulated its complete wavefield response (Figure 1D). To introduce a constrained heterogeneity, we added a single rough interface representing the weathered-bedrock boundary (Figure 1B). No other complexities, such as lateral velocity variations, elastic effects, or ground roll, were included to isolate the impact of topographic roughness on seismic wave propagation within an acoustic framework. The full wavefield simulation (Figure 1E) revealed that even a single rough interface generates distorted events.

To examine these effects separately, we conducted a near-surface-only simulation by retaining just the topographic interface and replacing the subsurface with a homogeneous medium (Figure 1C). This wavefield (Figure 1F) captures diffractions and multiples from the rough boundary but excludes deeper reflections. This "near-surface-only" wavefield serves as a reference for additive noise to be superimposed on the reflections of interest. By subtracting this near-surface-only wavefield from the full simulation, we isolated the net effect of topographic transmission on deeper reflections (Figure 1G). The result retains primary reflections with phase and amplitude distortions, providing a framework to analyze reflection distortions in detail.

Anatomy of distortions from rough interface

We constructed a series of synthetic models with increasing complexity to explore how near-surface roughness distorts seismic reflections. These models vary in the scale of topographic heterogeneity, allowing us to observe the evolution of wavefield distortions as roughness increases. The simulations use a Klauder wavelet with a frequency range of 2–50 Hz, while the near-surface layer is assigned a velocity of 740 m/s. Our starting point is a baseline model with a flat near-surface boundary and no topographic perturbations (Figure 3A). This unperturbed case yields clean wavefields (Figure 3G) with continuous reflectors and coherent phase behavior (Figure 3M) and serves as a reference for identifying distortions caused by surface irregularities.

We apply moderate topographic roughness to the bedrock interface using a von Kármán (1948) stochastic model, similar to the seabed roughness approach of Goff and Jordan (1988), to represent a realistic weathered-bedrock transition typical of land seismic environments. The interface follows a Gaussian-distributed surface height with a standard deviation σ = 10 m, correlation length L_0 = 12.5 m, and fractal exponent $\nu = 0.5$. Figure 2 conceptually illustrates key parameters, including the surface height (σ) and the dominant wavelength of lateral heterogeneity ($\boldsymbol{\lambda_c} = 2\pi L_0$), estimated as ~79 m**.** While the model incorporates a range of scales, we focus on this dominant wavelength for simplicity. Given a dominant seismic wavelength of ~30 m, this model represents a moderate level of near-surface heterogeneity. The resulting wavefield (Figure 3H) reveals tightly curved diffraction hyperbolas that cling to each reflector. These are not randomly scattered artifacts. Rather, they occur along the reflection paths and arise from the wave's interaction with the rough interface during transmission.

Figure 2 illustrates this reflection-induced distortion mechanism**.** As a seismic wave crosses a rough interface, localized irregularities act as secondary scatterers, generating diffractions that co-propagate with the primary reflection. These associated diffraction hyperbolas are tangential to the reflector, directly disrupting the continuity of the reflection event.

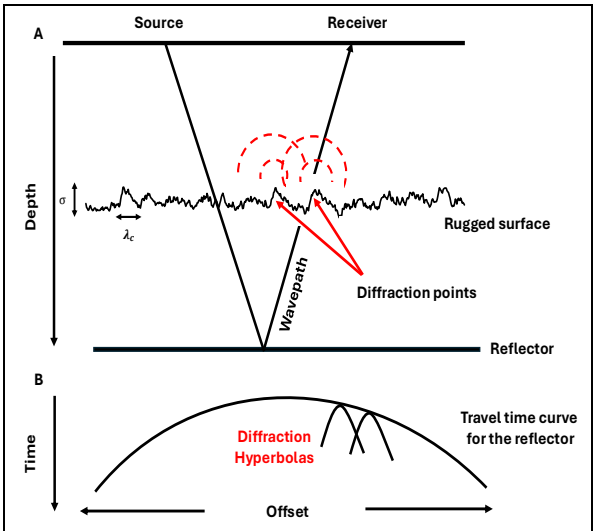

Figure 2: (A) seismic wave encounters a diffraction point along a rugged surface, generating a scattered wavefront (red dashed lines) that interferes with the primary reflection. (B) The resulting seismic events in the time domain exhibit diffraction hyperbolas that are tangential to the reflection. The diffraction events follow the reflection wavfront but exhibit much steeper moveouts.

10.1190/image2025-4316605.1

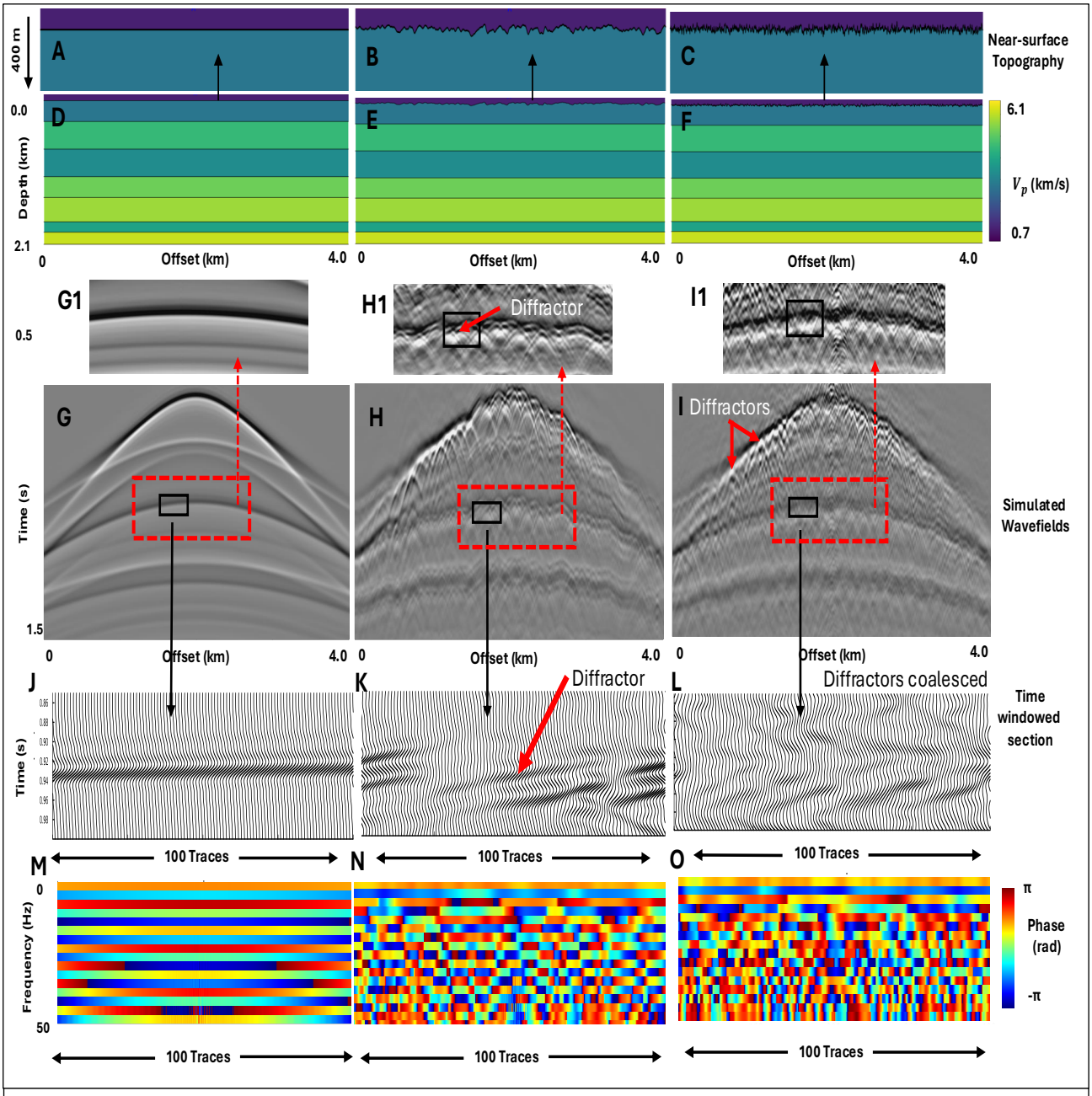

Figure 3. Progressive impact of near-surface topography on seismic reflections (derived as explained in Figure 1) and phases—from clean propagation to speckle noise.(A–C): Near-surface velocity models with increasing surface roughness: (A) smooth surface; (B) medium-scale topographic perturbations with characteristic heterogeneity scale $\lambda_c \approx 80$ m (larger than the dominant seismic wavelength); (C) small-scale perturbations with $\lambda_c \approx 10$ m (a fraction of the dominant wavelength). (D–F): Corresponding full velocity models with deeper layered structure beneath each near-surface realization. (G–I): Simulated seismic wavefields: (G) shows clean reflection hyperbolas; (H) shows reflections distorted by multiple diffraction events riding along the reflection path due to propagation distortion; (I) shows strong coalescing diffractions, clearly visible for shallow reflectors and no longer distinguishable for deeper ones. (J–L): Zoomed-in seismic traces revealing distortion anatomy at different scales. (M–O): Phase spectra across 100 traces: (M) shows coherent phase alignment; (N) shows increasing phase irregularity; (O) approaches full phase randomization typical of speckle noise from near-surface scattering.

10.1190/image2025-4316605.1

When multiple scatterers lie along the wave path, the distortion can intensify. Crucially, these are not generic noise artifacts; they exist only because the reflection exists. Without the reflection, these distortions would not appear. Nevertheless, we can identify individual diffractions, such as the one marked by the red arrow in the zoomed window (Figure 3K).

Interference between reflections and diffractions introduces localized phase distortions that intensify with frequency (Figure 3N). Although these disruptions appear irregular**,** their phase is distorted but not yet fully randomized. This suggests that, with sufficiently fine spatial sampling (e.g., the 2 m grid used in these examples), we may still be able to identify and incorporate these features into the velocity model. In the real world, however, where sampling intervals are typically 10-25 m, this coherence loss becomes much more difficult to capture, making accurate processing and phase correction far more challenging.

From diffraction to speckle: Phase randomization

As demonstrated, densely packed small-scale heterogeneities disrupt seismic wavefronts and severely degrade phase coherence. In this regime, seismic phases become fully randomized (Figure 3O), with distortions increasing with frequency. Lower frequencies retain more coherence, while higher frequencies exhibit pronounced phase scattering. The zoomed section in Figure 3L clearly shows the loss of deterministic structure at high frequencies. We also observe spatial homogenization of the distortion pattern: the statistical characteristics of the phase distortions appear consistent across different windows along the same reflector (Figure 3I). This uniformity signals the onset of a speckle noise regime, where local features are lost, and the wavefield becomes statistically stationary.

To quantify this, we apply circular statistical analysis (Mardia and Jupp, 2009) to the phase distributions. Figure 4 shows phase histograms at two frequencies, overlaid with corresponding von Mises distributions, a circular analog of Gaussian distributions for wrapped-phase data (Bakulin et al., 2024). In all cases, the phase distribution is symmetrically spread around the circular mean $\bar{\theta}$ (i.e., the center of the distribution expected for a scattering-free phase) and closely follows the von Mises form, confirming the statistical signature of speckle noise. The spread of each distribution is characterized by the circular variance (V) or concentration parameter (κ), both of which vary systematically with frequency. As expected from scattering physics, variance increases with frequency since shorter wavelengths experience more severe distortions when interacting with a fixed rough interface.

Crucially, the speckle observed in our study originates from transmission effects, which involve wavefronts interacting with rough near-surface topography before reaching the receivers. This transmission-induced speckle noise fundamentally limits coherent imaging, particularly for shallow reflectors, where the wavefield is most susceptible to surface-induced distortions.

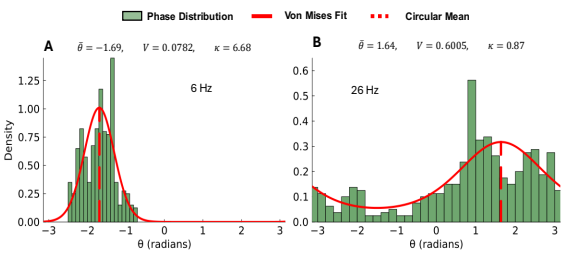

Figure 4: Frequency-dependent seismic phase distributions across 400 traces window affected by near-surface topography, computed within 100 ms window centered on the primary reflection: (A) At 6 Hz, the distribution peaks with low variance, indicating strong phase coherence and minimal interaction with near-surface roughness; (B) At 26 Hz, the distribution becomes highly dispersed with a variance of ~0.6, approaching a near-uniform distribution, typical of severe speckle noise, where coherent signal attributes are lost due to dense, fine-scale heterogeneity

Conclusions

We systematically investigated the distortions in land seismic data caused by complex near-surface conditions. Using advanced numerical modeling with finite-element code and adaptive meshing, we focused solely on a rough interface between weathered and bedrock layers at 100 meters depth as the source of heterogeneity. Our simulations revealed that a significant and persistent distortion arises from the propagation effects caused by reflections traveling through this rough near-surface boundary. These transmission-induced distortions impact all reflectors, whether deep or shallow, by generating diffractions that ride along the reflector paths. By varying the roughness scale, we visualized the transition from isolated diffraction hyperbolas at medium scales to a dense speckle regime at smaller scales, where diffractions coalesce and become indistinguishable even with fine spatial sampling (as tight as 2 meters).

This speckled regime mimics phenomena seen in optics and acoustics. We confirmed that such coalescence leads to phase randomization, with frequency-dependent spread increasing at higher frequencies. For broadband seismic data, this implies escalating phase instability with frequency. These reflection-induced propagation distortions present a key challenge for seismic imaging in areas with complex near-surface geology. Understanding their nature should drive the development of better seismic imaging techniques that mitigate these effects without necessarily requiring ultra-dense acquisition.

REFERENCES

Bakulin, A., I. Silvestrov and D. Neklyudov, 2020, Importance of phase guides from beamformed data for processing multi-channel data in highly scattering media: The Journal of the Acoustical Society of America, **147**, no. 6, EL447–EL452.

Bakulin, A., D. Neklyudov and I. Silvestrov, 2022a, Seismic speckle as multiplicative noise explaining land reflections distorted by near-surface scattering: SEG International Exposition and Annual Meeting, D011S137R001. SEG.

Bakulin, A., D. Neklyudov, and I. Silvestrov, 2022b, Multiplicative seismic noise caused by small-scale near-surface scattering and its transformation during stacking: Geophysics, **87**, no. 5, V419–V435, doi: https://doi.org/10.1190/geo2021-0830.1.

Bakulin, A., D. Neklyudov and I. Silvestrov, 2024, The impact of receiver arrays on suppressing seismic speckle scattering noise caused by the meter-scale near-surface heterogeneity: Geophysics, **89**, no. 6, V551–V561, doi: https://doi.org/10.1190/geo2023-0489.1.

Badger, J., 2024a, Scalable DPG multigrid solver with applications in high-frequency wave propagation: PhD Thesis, University of Texas at Austin.

Badger, J., A. Bakulin, and S. Fomel, 2024b, Scalable, efficient, and adaptive simulation of frequency-domain wave propagation: SEG Technical Program Expanded Abstracts, 1796–1800, doi: https://doi.org/10.1190/image2024-4101625.1

Goff, J. A. and T. H. Jordan, 1988, Stochastic modeling of seafloor morphology: Inversion of sea beam data for second-order statistics: Journal of Geophysical Research: Solid Earth, **93**, no. B11, 13589–13608.

Goodman, J. W., 2015. Statistical optics: John Wiley and Sons.

Mardia, K. V. and P. E. Jupp, 2009. Directional statistics: John Wiley and Sons.

Phillips, J. D., L. Pawlik and P. Šamonil, 2019. Weathering fronts: Earth-Science Reviews, **198**, 102925.

Stork, C., 2020. How does the thin near surface of the earth produce 10–100 times more noise on land seismic data than on marine data? First Break, **38**, no. 8, 67–75.

Stork, C., 2024. Understanding land seismic scattering noise through careful simulation. First Break, **42**, no. 1, 85–89.

Von Karman, T., 1948. Progress in the statistical theory of turbulence: Proceedings of the National Academy of Sciences, **34**, no. 11, 530–539.

Yilmaz, Ö., 2001. Seismic data analysis: Processing, inversion, and interpretation of seismic data: Society of Exploration Geophysicists.